JOURNAL OF BACTERIOLOGY, Jan. 1997, p. 453–462 Vol. 179, No. 2
0021-9193/97/$04.00+0

The VirB4 ATPase of *Agrobacterium tumefaciens* Is a Cytoplasmic Membrane Protein Exposed at the Periplasmic Surface

TU ANH T. DANG AND PETER J. CHRISTIE*

Department of Microbiology and Molecular Genetics, The University of Texas Health Science Center at Houston, Houston, Texas 77030

Received 26 June 1996/Accepted 1 November 1996

The VirB4 ATPase of *Agrobacterium tumefaciens*, a putative component of the T-complex transport apparatus, associates with the cytoplasmic membrane independently of other products of the Ti plasmid. VirB4 was resistant to extraction from membranes of wild-type strain A348 or a Ti-plasmidless strain expressing *virB4* from an IncP replicon. To evaluate the membrane topology of VirB4, a nested deletion method was used to generate a high frequency of random fusions between *virB4* and *'phoA*, which encodes a periplasmically active alkaline phosphatase (AP) deleted of its signal sequence. VirB4::PhoA hybrid proteins exhibiting AP activity in *Escherichia coli* and *A. tumefaciens* had junction sites that mapped to two regions, between residues 58 and 84 (region 1) and between residues 450 and 514 (region 2). Conversely, VirB4::β-galactosidase hybrid proteins with junction sites mapping to regions 1 and 2 exhibited low β-galactosidase activities and hybrid proteins with junction sites elsewhere exhibited high β-galactosidase activities. Enzymatically active VirB5::PhoA hybrid proteins had junction sites that were distributed throughout the length of the protein. Proteinase K treatment of *A. tumefaciens* spheroplasts resulted in the disappearance of the 87-kDa VirB4 protein and the concomitant appearance of two immunoreactive species of ~35 and ~45 kDa. Taken together, our data support a model in which VirB4 is topologically configured as an integral cytoplasmic membrane protein with two periplasmic domains.

Agrobacterium tumefaciens is a plant pathogen with the unique ability to deliver oncogenes to the genomes of susceptible plants cells (for reviews, see references 27 and 64). The translocation-competent form of the transferred DNA (T-DNA) has been proposed to consist of a single-stranded molecule covalently associated at its 5′ end with the VirD2 protein and noncovalently associated along its length with VirE2, a single-stranded-DNA-binding protein (14, 64). Delivery of these so-called T-complexes across the *A. tumefaciens* envelope requires 10 of the 11 products of the *virB* operon and the product of the *virD4* gene (5, 8). Three proposed components of the T-complex transport machinery, VirB4, VirB11, and VirD4, contain consensus Walker A nucleotide-binding motifs. Mutational analyses have established that VirB4 and VirB11 require intact nucleoside triphosphate (NTP)-binding motifs to function as virulence factors (7, 22, 40, 51). Similar results have been obtained for the VirD4 homolog TraG of the IncP plasmid RP4 (4). VirB4 and VirB11 have been shown to exhibit weak ATPase activities (13, 45). Purified VirB11 also autophosphorylates, although the physiological relevance of this in vitro activity remains to be demonstrated (13).

Recent sequence comparisons indicate that the VirB and VirD4 proteins are highly similar to components of conjugation systems dedicated to the interbacterial transmission of broad-host-range (BHR) plasmids of the IncN (pKM101) (39), IncP (RP4) (30), and IncW (R388) (27) incompatibility groups and, to a lesser extent, the *Escherichia coli* F plasmid (31). These findings have provided strong support for an early hypothesis that *A. tumefaciens* delivers T-complexes to plants by a process resembling conjugation (50). More intriguingly, most of the VirB proteins are highly similar to components of the Ptl transport machinery dedicated to export of the six-subunit pertussis toxin across the *Bordetella pertussis* envelope (60, 61). Furthermore, the VirB4 homolog PicB of *Helicobacter pylori* has been postulated to function in the export across the bacterial envelope of an unidentified product that is responsible for induction of interleukin-8 secretion in gastric epithelial cells (54). VirB11-like proteins constitute a large family of ATPases whose functions are required for conjugal transfer of DNA, export of a variety of protein substrates, and import of DNA by transformation (see reference 31). Together, these discoveries underscore the general importance of activities provided by proteins related to the VirB4, VirB11, and VirD4 ATPases for macromolecular transport of DNA or protein across the gram-negative envelope. In fact, the T-complex transport machinery itself recognizes and delivers a variety of substrates, including T-DNA, the mobilizable IncQ plasmids, and possibly VirE2 protein only, to competent bacterial or plant recipient cells. VirB4, VirB11, and VirD4 are required for the export of each of these molecules (5, 7–9, 13, 14, 22, 58).

The precise contributions of the VirB4, VirB11, and VirD4 proteins to transport have not been elucidated. Topology studies indicate that VirD4 possesses a transmembrane configuration (37), whereas VirB11 likely resides exclusively at the cytoplasmic face of the cytoplasmic membrane (18, 40). VirB4 possesses several hydrophobic regions of sufficient length to span the membrane, but each of these regions is interrupted by at least one and in some cases several charged residues (29, 46, 53, 56, 57). These findings have led to contradictory predictions that VirB4 resides in the cytosol (63) or in the periplasmic

* Corresponding author. Mailing address: Department of Microbiology and Molecular Genetics, The University of Texas Health Science Center at Houston, 6431 Fannin, Houston, TX 77030. Phone: (713) 794-1744, ext. 1518. Fax: (713) 794-1782. E-mail: christie@utmmg.med.uth.tmc.edu.

space (6). Previously, we demonstrated that VirB4 cofractionates predominantly with the cytoplasmic membranes of wild-type strain A348 and cells expressing *virB4* in the absence of other *virB* genes (7). In this study, we further characterized the nature of the membrane association of VirB4. Our results are consistent with a model in which VirB4 possesses two periplasmic domains, one near its N terminus and a second just after a Walker A NTP-binding motif.

MATERIALS AND METHODS

Enzymes and reagents. Isopropyl-β-D-thiogalactopyranoside (IPTG), phenylmethylsulfonyl fluoride (PMSF), 5-bromo-4-chloro-3-indolyl phosphate (XP), 5-bromo-4-chloro-3-indolyl-β-D-galactopyranoside (X-Gal), *p*-nitrophenyl phosphate, *o*-nitrophenyl galactoside, Triton X-100, Triton X-114, carbenicillin, kanamycin, and tetracycline were purchased from Sigma (St. Louis, Mo.). *p*-Nitroblue tetrazolium and alkaline phosphatase (AP)-conjugated goat anti-rabbit immunoglobulin G were from Bio-Rad Laboratories (Hercules, Calif.). Acetosyringone (3′,5′-dimethoxy-4′-hydroxyacetophenone [AS]) was from Aldrich (Milwaukee, Wis.). Restriction endonucleases were from New England Biolabs (Beverly, Mass.), Promega (Madison, Wis.), or Gibco-BRL (Grand Island, N.Y.). Exonuclease III was from United States Biochemical (Cleveland, Ohio). S1 nuclease and the four deoxyribonucleoside triphosphates were from Boehringer Mannheim (Indianapolis, Ind.). Klenow fragment of *E. coli* DNA polymerase I was from Promega.

Bacterial strains, plasmids, and growth conditions. Table 1 lists the bacterial strains and plasmids used in this study and their relevant characteristics. Conditions for growth of *E. coli* and *A. tumefaciens* cells have been previously described (14). For induction of the *vir* genes, *A. tumefaciens* cells were grown in MG/L medium (49) to an optical density at 600 nm (OD_{600}) of 0.5, harvested by centrifugation, and inoculated at an initial OD_{600} of 0.2 into IM medium (AB minimal medium [pH 5.5] containing 1 mM phosphate [13]) supplemented with 200 μM AS. Cultures were incubated with shaking at 28°C for 18 h and then harvested for protein analysis (13). In *A. tumefaciens* and *E. coli* cells, plasmids were maintained by addition of carbenicillin (50 μg/ml), kanamycin (50 μg/ml), or tetracycline (5 μg/ml) to the growth medium.

Recombinant DNA techniques. DNA manipulations and DNA electrophoresis were performed as described by Sambrook et al. (41). *A. tumefaciens* cells were transformed by electroporation, and plasmids were recovered for physical characterization as previously described (8). DNA sequencing was carried out at the DNA Core Facility of the Department of Microbiology and Molecular Genetics, University of Texas—Houston Medical School, with an ABI 373A DNA sequencer (Perkin-Elmer, Applied Biosystems Division), using *Taq* polymerase in a thermal cycling reaction. PCR amplification was performed with a Perkin-Elmer Cetus DNA thermocycler, using *Taq* DNA polymerase from Promega. Oligonucleotides were synthesized with a BioSearch 8600 DNA synthesizer.

Protein analysis and immunoblotting. Proteins were resolved by sodium dodecyl sulfate-polyacrylamide gel electrophoresis (SDS-PAGE) as previously described (8). VirB proteins, DnaA, and VirB::PhoA hybrid proteins were visualized by SDS-PAGE; protein was then transferred to nitrocellulose membranes, and immunoblot development was achieved with goat anti-rabbit antibodies conjugated to AP (14). Previous studies established the reactivity of antisera to the VirB4 (58), VirB5 (7), VirB11 (13), DnaA (18, 34), and VirA (62) proteins.

Subcellular fractionation. *E. coli* and *A. tumefaciens* total cell extracts were prepared by cell lysis with a French pressure cell (14,000 lb/in^2) followed by removal of cell debris and unbroken cells by low-speed centrifugation at 7,000 × *g*. The cleared lysate was separated into soluble (cytoplasmic and periplasmic) and insoluble (membrane) materials by centrifugation at 200,000 × *g* for 1 h at 4°C with an SW55 rotor. For solubilization studies, total membrane fractions were washed with 0.2 M KCl and then suspended in 10 mM Tris buffer (pH 8.0) containing one of the following: 0.5 or 1 M NaCl, 1 M KCl, 10 mM EDTA, $NaHCO_3$ adjusted to a pH of 3.0 or 11.0, 5 M urea, 1 or 2% Triton X-100, 1% SDS, 1 or 2% Triton X-114, or 1 or 2% octylglucoside (OG) (24). The final concentration of protein in each reaction mixture was 1 mg/ml. Reaction mixtures were incubated at 4°C for 1 h and then centrifuged at 100,000 × *g* for 30 min to pellet insoluble material. This material was resuspended in 10 mM Tris buffer (pH 8.0) to a volume equal to that of the soluble material. Soluble and insoluble materials were electrophoresed through SDS-polyacrylamide gels and assayed for the presence of the VirB4 and VirB5 proteins by immunoblot analysis. Treated membranes were further fractionated into cytoplasmic and outer membrane fractions by isopycnic sucrose density gradient centrifugation at 120,000 × *g* and 4°C as previously described (14). The efficiency of membrane separation was monitored by assaying gradient fractions for the presence of the cytoplasmic membrane markers VirA (62) and NADH oxidase activity (see reference 18) and by measuring the OD_{280} for total protein content. The presence of VirB4 in gradient fractions was assessed by SDS-PAGE and immunostaining.

In vitro construction of *virB4*::*phoA* and *virB5*::*phoA* gene fusions by exonuclease III nested deletions. The *′phoA* gene, which encodes AP lacking its signal sequence, was isolated from plasmid pUI1156 as an *Xba*I-*Kpn*I fragment and introduced into corresponding sites of pPC948, resulting in plasmid pPC103. Next, the *virB4*, *virB5*, and *′phoA* genes from pPC103 were isolated as a ~4.4-kb *Nde*I-*Kpn*I fragment and introduced into similarly digested pBSIISK$^+$*Nde*I. The resulting plasmid, pPC104, was used to construct a collection of *virB4*::*phoA* and *virB5*::*phoA* chimeric genes. This was achieved by cleaving pPC104 at unique *Bsu*36I (5′ overhang) and *Sac*I (3′ overhang) sites to generate ends that were susceptible and resistant, respectively, to digestion with exonuclease III. In preliminary experiments, the exonuclease III digestion reaction was estimated to proceed at approximately 250 bases per min at 37°C. Linearized pPC104 was resuspended in exonuclease III buffer and incubated at 37°C. Exonuclease III was added at time zero, and then a total of 25 aliquots were removed at intervals of 30 s and placed immediately into S1 nuclease-containing tubes on ice. After all samples were collected, the tubes were placed at room temperature for 30 min; this was followed by addition of S1 stop buffer. The ends of the treated DNA were converted to blunt ends by incubation with the Klenow fragment of *E. coli* DNA polymerase I and deoxynucleoside triphosphates at room temperature for 30 min. The 25 samples were pooled into five groups, each containing aliquots from five consecutive time points. The linear DNA from each of the five groups was isolated from a 1% NuSieve GTG agarose gel, ends were ligated together with T4 DNA ligase, and recircularized plasmid DNA was introduced by electroporation into *E. coli* CC118 cells. Transformants producing in-frame fusions to AP were screened on Luria-Bertani (LB) plates containing the chromogenic indicator XP at 40 μg/ml (34). A total of 32 independent *virB4*::*phoA* fusions and 10 independent *virB5*::*phoA* fusions were identified by physical mapping with restriction enzymes. Fusion junctions were mapped by DNA sequence analysis with the sequencing primer 5′-ACCGCCGGGTGCACTAATAT-3′, which is complementary to the 5′ end of the *′phoA* gene.

In vitro construction of *virB4*::*phoA* gene fusions by cloning. Three *virB4*::*phoA* gene fusions were constructed by insertion of *′phoA* cassettes into unique restriction sites in the *virB4* coding sequence carried on pPC943, as described in Table 1.

Construction of *virB4*::*lacZ* fusions. Plasmids expressing *virB4*::*lacZ* fusions from P_{lac} were constructed by the following methods. The *Bam*HI fragment containing the *lacZ* cassette from pMC1871 was subcloned into pBCSK$^+$ to generate pTAD250. Next, the *Xba*I-*Kpn*I fragment containing the *lacZ* cassette from pTAD250 was substituted for an *Xba*I-*Kpn*I fragment containing the *′phoA* gene in plasmids expressing *virB4*::*phoA* fusions generated by the exonuclease III nested-deletion method. Plasmids were transformed into *E. coli* DH5α cells and plated on LB plates containing carbenicillin (50 μg/ml) and the chromogenic indicator X-Gal (40 μg/ml). Analysis of transformants appearing as white or light-blue colonies led to identification of pTAD262 (*virB4*::*lacZ58*), pTAD263 (*virB4*::*lacZ76*), pTAD264 (*virB4*::*lacZ84*), pTAD265 (*virB4*::*lacZ450*), pTAD267 (*virB4*::*lacZ487*), and pTAD268 (*virB4*::*lacZ514*).

Two *virB4*::*lacZ* gene fusions with junction sites corresponding to residues 237 and 780 of VirB4 were constructed as described in Table 1. *E. coli* and *A. tumefaciens* expressing *virB4*::*lacZ237* and *virB4*::*lacZ778* grew as dark-blue colonies on plates containing X-Gal.

Enzyme assays. *E. coli* cells expressing the gene fusions were grown in LB broth (41) to an OD_{600} of 0.4; IPTG was then added to a final concentration of 1 mM, and cells were incubated for an additional 1 h at 37°C. *A. tumefaciens* A348 cells expressing the gene fusions were grown to an OD_{600} of 0.4 in MG/L broth. Cultures were also incubated for 18 h in *vir* gene induction media (IM) with or without 200 μM AS (18). Iodoacetamide (1 mM final concentration) was routinely added to cell cultures prior to harvesting to prevent disulfide bond formation and thus the spontaneous activation of cytoplasmically localized AP (17). AP and β-galactosidase (β-Gal) activities were assayed in permeabilized cells as described by Manoil (33) and Miller (35). Units of activity were calculated according to the references mentioned above. At least three independent assays were performed in triplicate for each strain.

Protease susceptibility studies. *A. tumefaciens* whole cells and spheroplasts were prepared for treatment with proteinase K as previously described (18). The susceptibility of proteins in whole cells and spheroplasts to protease was determined by the addition of proteinase K at a final concentration of 100, 200, or 400 μg/ml and incubation on ice for 45 min. The proteolysis reaction was quenched by the addition of 2 mM PMSF followed by incubation on ice for 5 min. To monitor protease susceptibility of proteins in lysed spheroplasts, spheroplasts were treated with 0.5% Triton X-114 as previously described (18). The extent of proteolysis of VirB4, VirB5, VirB11, and DnaA was analyzed by SDS-PAGE and immunostaining with antibodies specific to these proteins.

RESULTS

Nature of membrane association of VirB4. VirB4 cofractionates in sucrose density gradients with the cytoplasmic membranes of wild-type strain A348 as well as A136(pZDH10), a Ti-plasmidless strain that constitutively expresses *virB4* and *virB5* from P_{lac} on an IncP replicon (7). The nature of the membrane association of VirB4 was further examined by testing for extractability from membranes of A348 cells with various reagents. Figure 1A shows that VirB4 was detected exclu-

TABLE 1. Bacterial strains and plasmids used in this study

Bacterial strain or plasmid	Relevant characteristics	Source or reference
Strains		
E. coli		
DH5α	λ⁻ ϕ80d/*lacZ*Δ*M15*Δ(*lacZYA-argF*)*U169recA1 endA1 hsdR17*(r_K^- m_K^+) *supE44 thi-1 gyrA relA1*	41
CC118	*araD139* Δ(*ara leu*)*7697* Δ*lacX74 phoAD20 galE galK thi rpsE rpoB argE*(Am) *recAI*	33
A. tumefaciens		
A136	Strain C58 cured of pTiC58	59
A348	A136 containing octopine-type Ti plasmid pTiA6NC	23
PC1004	Formerly A348Δ*virB4*; A348 derivative sustaining a *virB4* gene deletion from pTiA6NC	8
Plasmid vectors		
pBIISK⁺	Crb^r; cloning vector	Stratagene
pBCSK⁺	Chl^r; cloning vector	Stratagene
pBSIISK⁺*Nde*I	Crb^r; pBSIISK⁺ containing an *Nde*I restriction site at the translational start site of *lacZ*	8
pBKSK⁺*Nde*I	Kan^r; pBCSK⁺ containing an *Nde*I restriction site at the translational start site of *lacZ*	8
pMC1871	Tet^r; β-Gal translational fusion vector derived from pBR322 containing a promoterless *lacZ* gene lacking a ribosome binding site and the first eight nonessential N-terminal amino acid codons; contains multiple cloning sites on either side of the *lacZ* gene	Pharmacia Biotech
pUI1156	Crb^r; pBSIIKS⁺ carrying *′phoA* from pUI310 introduced as an *Xba*I and *Sac*I fragment; *′phoA* is in reading frame one with respect to upstream polylinker sequence	M. Wood and S. Kaplan
pUI1158	Crb^r; pBSIIKS⁺ carrying *′phoA* from pUI310 introduced as an *Xba*I and *Sac*I fragment; *′phoA* is in reading frame two with respect to upstream polylinker sequence	M. Wood and S. Kaplan
pUI1160	Crb^r; pBSIIKS⁺ carrying *′phoA* from pUI320 introduced as an *Xba*I and *Sac*I fragment; *′phoA* is in reading frame three with respect to upstream polylinker sequence	J. Eraso and S. Kaplan
pSW172	Tet^r; BHR IncP plasmid containing P_{lac} and polylinker sequence from pIC19	12
pLAFR2	Tet^r; cosmid vector with *mob* site and *oriT* of RK2; carries the entire *lac* operon on a *Bam*HI fragment	G. Weinstock
pZDM10	Crb^r; pBSIIKS⁺ with *virB4* gene under P_{lac} control	7
pZDH10	Crb^r Tet^r; pZDM10 ligated to pSW172 at *Sac*I site	7
pPC103	Chl^r; pPC945 carrying *′phoA* from pUI1156 as an *Xba*I-*Kpn*I fragment introduced downstream of *virB5*	This study
pPC104	Crb^r; pBSIISK⁺ *Nde*I carrying *virB4*, *virB5*, and *phoA* genes introduced as a 4.4-kb *Nde*I-*Kpn*I fragment from pPC103 downstream of P_{lac}	This study
pPC943	Kan^r; pBKSK⁺*Nde*I with the *virB4* and *virB5* genes introduced as a 2.09-kb *Nde*I-*Sac*I fragment from pPC947 (8) downstream of P_{lac}	This study
pPC945	Chl^r; pBCSK⁺*Nde*I with the *virB4* and *virB5* genes introduced as a 2.09-kb *Nde*I-*Sac*I fragment from pPC947 (8) downstream of P_{lac}	This study
pPC953	Kan^r; pBKSK⁺*Nde*I expressing *virB5* from P_{lac}	8
pTAD45	Kan^r; pBKSK⁺*Nde*I containing bp 1 to 1834 of *virB4* downstream of P_{lac} by introduction of an *Nde*I-*Pst*I fragment from pPC945	This study
pTAD46	Kan^r; pBKSK⁺*Nde*I containing bp 1 to 937 of *virB4* downstream of P_{lac} by introduction of an *Nde*I-*Eco*RI fragment from pPC945	This study
pTAD47	Kan^r; pBKSK⁺*Nde*I containing bp 1 to 705 of *virB4* downstream of P_{lac} by introduction of an *Nde*I-*Bam*HI fragment from pPC945	This study
pTAD58	Kan^r; pBKSK⁺*Nde*I containing the *virB4*::*phoA237* gene fusion downstream of P_{lac}, with *′phoA*, carried on a 2.2-kb *Bam*HI-*Kpn*I fragment from pUI1158, substituted for a *Bam*HI-*Kpn*I fragment carrying 1.66 kb of the 3′ end of *virB4* in pPC943	This study
pTAD59	Kan^r; pBKSK⁺*Nde*I containing the *virB4*::*phoA250* gene fusion downstream of P_{lac}, with *′phoA*, carried on a 2.2-kb *Eco*RV-*Kpn*I fragment from pUI1156, substituted for an *Sph*I (made blunt-ended with T4 DNA polymerase)-*Kpn*I fragment carrying 1.62 kb of the 3′ end of *virB4* in pPC943	This study
pTAD60	Kan^r; pBKSK⁺*Nde*I containing the *virB4*::*phoA312* gene fusion downstream of P_{lac}, with *′phoA*, carried on a 2.2-kb *Eco*RI-*Kpn*I fragment from pUI1158, substituted for an *Eco*RI-*Kpn*I fragment carrying 1.43 kb of the 3′ end of *virB4* in pPC943	This study
pTAD100	Kan^r Tet^r; pPC943 ligated at the *Aat*II site within *virB5* to the *Eco*RV site of pSW172; expresses *virB4* from P_{lac}	This study
pTAD140	Crb^r; pBSIISK⁺*Nde*I containing bp 1 to 2340 of *virB4* downstream of P_{lac} by introduction of an *Nde*I-*Eco*RI fragment from a partial digest of pPC945	This study
pTAD250	Chl^r; pBCSK⁺ with the *lacZ* gene introduced as a 3.2-kb *Bam*HI fragment from pMC1871	This study
pTAD261	Kan^r; pBKSK⁺*Nde*I containing the *virB4*::*lacZ237* gene fusion downstream of P_{lac}, with *lacZ*, carried on a 3.9-kb *Sma*III-*Hin*dIII (made blunt-ended with the Klenow fragment of DNA polymerase I) fragment from pMC1871, introduced into the *Eco*RV site in the pBluescript polylinker just downstream of the *virB4* coding sequence in pTAD47	This study
pTAD262	Crb^r; pBSIISK⁺*Nde*I containing the *virB4*::*lacZ58* gene fusion downstream of P_{lac}, with *lacZ*, carried on a 3.2-kb *Xba*I-*Kpn*I fragment from pTAD250, substituted for *′phoA* in the *virB4*::*phoA58* gene fusion obtained from exonuclease III nested deletion	This study

Continued on following page

TABLE 1—*Continued.*

Bacterial strain or plasmid	Relevant characteristics	Source or reference
pTAD263	Crb^r; pBSIISK$^+$*Nde*I containing the *virB4*::*lacZ76* gene fusion downstream of P_{lac}, with *lacZ*, carried on a 3.2-kb *Xba*I-*Kpn*I fragment from pTAD250, substituted for *'phoA* in the *virB4*::*phoA76* gene fusion obtained from exonuclease III nested deletion	This study
pTAD264	Crb^r; pBSIISK$^+$*Nde*I containing the *virB4*::*lacZ84* gene fusion downstream of P_{lac}, with *lacZ* gene, carried on a 3.2-kb *Xba*I-*Kpn*I fragment from pTAD250, substituted for *'phoA* in the *virB4*::*phoA84* gene fusion obtained from exonuclease III nested deletion	This study
pTAD265	Crb^r; pBSIISK$^+$*Nde*I containing the *virB4*::*lacZ450* gene fusion downstream of P_{lac}, with *lacZ*, carried on a 3.2-kb *Xba*I-*Kpn*I fragment from pTAD250, substituted for *'phoA* in the *virB4*::*phoA450* gene fusion obtained from exonuclease III nested deletion	This study
pTAD267	Crb^r; pBSIISK$^+$*Nde*I containing the *virB4*::*lacZ487* gene fusion downstream of P_{lac}, with *lacZ*, carried on a 3.2-kb *Xba*I-*Kpn*I fragment from pTAD250, substituted for *'phoA* in the *virB4*::*phoA487* gene fusion obtained from exonuclease III nested deletion	This study
pTAD268	Crb^r; pBSIISK$^+$*Nde*I containing the *virB4*::*lacZ514* gene fusion downstream of P_{lac}, with *lacZ*, carried on a 3.2-kb *Xba*I-*Kpn*I fragment from pTAD250, substituted for *'phoA* in the *virB4*::*phoA514* gene fusion obtained from exonuclease III nested deletion	This study
pTAD270	Crb^r; pBSIISK$^+$*Nde*I containing the *virB4*::*lacZ780* gene fusion downstream of P_{lac}, with *lacZ*, carried on a 3.9-kb *Sma*III-*Hin*dIII (made blunt-ended with the Klenow fragment of DNA polymerase I) fragment from pMC1871, introduced at the *Eco*RV site in the pBluescript polylinker just downstream of the *virB4* coding sequence in pTAD140	This study

sively in the particulate fractions upon centrifugation of membranes treated with a reagent (or under a condition) effective at disrupting electrostatic interactions, e.g., NaCl, KCl, EDTA, or basic (pH 11) or acidic (pH 3) conditions, or with a protein denaturant, e.g., 5 M urea. Interestingly, VirB4 also was found in the particulate fractions after treatment with a nonionic detergent, e.g., Triton X-100, Triton X-114, or OG (Fig. 1B) (see below). We have shown elsewhere that the integral cytoplasmic membrane protein VirA (62) also sediments with the particulate materials after treatment of A348 membranes with any one of these reagents (40).

Next, to distinguish whether particulate VirB4 recovered from the membrane treatments was membrane-associated or aggregated protein, we centrifuged the insoluble material through isopycnic sucrose gradients and assayed fractions for the presence of VirB4 and the cytoplasmic membrane markers VirA and NADH oxidase activity. Figure 2 shows representative fractionation profiles obtained from sucrose density centrifugation of treated A348 membranes from uninduced and AS-induced cells. Treatments with NaCl or urea resulted in partitioning of VirB4 in low-density fractions near the tops of the gradients. These fractions also contained cytoplasmic membrane, as evidenced by copartitioning of the cytoplasmic membrane markers VirA and NADH oxidase activity (data not shown). Thus, NaCl and urea treatments failed to extract VirB4 from the cytoplasmic membrane. Similar patterns of distribution were observed upon sucrose gradient analysis of membranes treated with the other reagents listed at the top of Fig. 1A. AS induction had no detectable effect on VirB4 partitioning in these gradients, suggesting that the *vir* gene products do not markedly influence the membrane association of VirB4.

In contrast to the above-mentioned findings, Triton X-100 treatment of membranes caused VirB4 (Fig. 2) and VirA (data not shown) to partition near the bottoms of the sucrose gradients. The absence of VirA from the low-density fractions, in

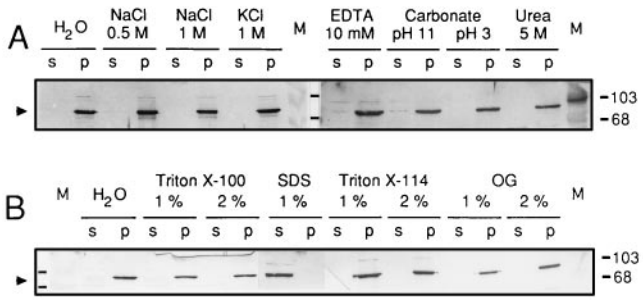

FIG. 1. Extractability of membrane-bound VirB4 protein. Total membranes from AS-induced A348 cells were concentrated by centrifugation and incubated with various reagents or under various conditions (A) or with detergents (B). Soluble (s) and particulate (p) material was separated by centrifugation and analyzed by SDS-PAGE and immunoblotting for the presence of VirB4 protein. The position of VirB4 is indicated by an arrowhead at the left. M, molecular mass markers (with sizes indicated at the right). Dashes in the center in panel A and at the left in panel B identify molecular mass markers with sizes of 103 and 68 kDa.

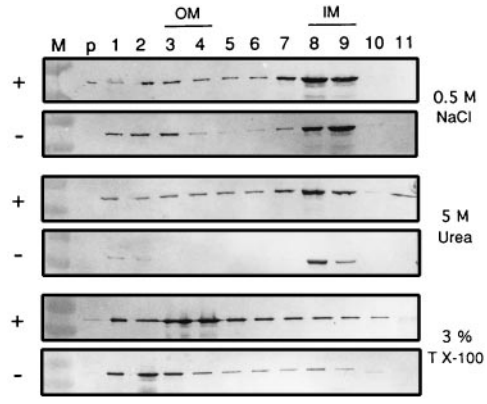

FIG. 2. Distribution of VirB4 in sucrose density gradients upon centrifugation of membranes treated with 0.5 M NaCl, 5 M urea, or 3% Triton X-100. Treated membranes from AS-induced (+) and uninduced (−) A348(pZDH10) cells were analyzed. Material at the bottom of the gradient (p) and fractions numbered 1 to 11 (bottom to top of gradients) were analyzed by SDS-PAGE and immunoblotting for the presence of VirB4. OM and IM correspond to fractions in which outer and cytoplasmic membranes, respectively, from untreated membranes were expected to distribute on the basis of sucrose densities of these fractions (see the text and references 14 and 18).

which untreated cytoplasmic membranes of *A. tumefaciens* normally partition (see reference 18), suggests that the detergent treatments effectively solubilized the cytoplasmic membrane. The observed patterns of distribution most probably can be explained by density shifts caused by binding of detergent to these proteins or detergent-induced protein aggregation.

Active *virB4*::*phoA* and *virB5*::*phoA* fusions generated by exonuclease III nested deletion. Results of the membrane treatment and fractionation studies suggested that VirB4 associates tightly with the cytoplasmic membrane. To evaluate the membrane topology of VirB4, we constructed in-frame fusions between *virB4* and *'phoA*, whose product, AP, folds into an active conformation only when secreted (33). Previous PhoA fusion studies using Tn*phoA* failed to identify active fusions between PhoA and VirB4 or its IncN homolog, TraB, suggesting that these proteins do not contain large periplasmic domains (6, 39). Because Tn*phoA* exhibits some site preference and does not always saturate a gene of interest, we utilized a nested-deletion method originally devised by Sugiyama et al. (52) for construction of in-frame gene fusions. We included *virB5* in these investigations to test the utility of this approach, since we (18) and others (6) had already provided evidence that VirB5 possesses exported domains.

Plasmids from 42 *E. coli* transformants that grew as blue colonies on XP-containing plates were isolated, and the fusion junctions were sequenced. Figures 3A and 4A show the junction points between *'phoA* and the *virB4* and *virB5* genes that yielded hybrid proteins with AP activity. Thirty-two of the sequenced products had in-frame *virB4*::*phoA* gene fusions with junction sites that mapped to 16 different positions clustered in two distinct regions of *virB4*. Region 1 corresponded to residues 58 to 84 near the amino terminus of VirB4, and region 2 corresponded to residues 450 to 514 in the middle of VirB4. As depicted in Fig. 3A, stretches of hydrophobic residues of sufficient length to span the cytoplasmic membrane flanked both regions. The remaining 10 plasmids possessed in-frame *virB5*::*phoA* gene fusions with junction sites that mapped to nine different positions; these junction sites were distributed along the length of *virB5* (Fig. 4A).

Twenty-five plasmids containing unique *virB4*::*phoA* and *virB5*::*phoA* gene fusions whose products exhibited AP activity in *E. coli* were ligated to the BHR plasmid pSW172 (12) for introduction into *A. tumefaciens* A348 cells. *A. tumefaciens* cells carrying these constructs, but not untransformed cells, grew as blue colonies on MG/L plates containing XP. Quantitative assays showed that *E. coli* and *A. tumefaciens* cells synthesizing the VirB4::PhoA and VirB5::PhoA hybrid proteins exhibited AP activities well above the background level of <2 U per OD_{600} unit reproducibly obtained for CC118 and A348 host cells (Fig. 3B and 4B). These analyses further showed that *E. coli* and *A. tumefaciens* cells synthesizing VirB5::PhoA hybrid proteins exhibited much higher AP activities than cells synthesizing VirB4::PhoA hybrid proteins. The VirB5::PhoA proteins generally gave rise to AP activities of between 800 and 2,000 U in both species. By contrast, the VirB4::PhoA proteins that mapped to region 1 gave rise to AP activities of 75 to 200 U in *E. coli* and 10 to 50 U in *A. tumefaciens*. The VirB4::PhoA proteins that mapped to region 2 gave rise to AP activities of 15 to 50 U in both species. The one exception, the hybrid protein with a junction point at residue 450, gave rise to higher AP activities of 150 to 175 U. We further quantitated the AP activities of *A. tumefaciens* cells incubated in IM only and in IM with 200 μM AS for induction of *vir* genes. All strains incubated in these media exhibited AP activities that were comparable to levels observed upon growth in MG/L media, indicating that the presence of Vir proteins does not contribute markedly to the stabilization of these hybrid proteins.

The nested-deletion method used in this study is predicted to generate in-frame *virB*::*phoA* fusions at a frequency of one in three for the religated plasmids. This high frequency likely accounts for our ability to recover active VirB5::PhoA hybrid proteins with junction points that mapped at intervals of 8 to 49 residues throughout the length of VirB5 (Fig. 4A). Therefore, we expected that a large number of the original *E. coli* transformants that grew as white colonies on XP plates synthesized inactive fusion proteins. To test for activity of hybrid proteins with junction points outside of regions 1 and 2, we constructed three *virB4*::*phoA* gene fusions that coded for hybrid proteins joined at residues 237, 250, and 312 of VirB4 (Fig. 3A). *E. coli* CC118 cells carrying plasmids pTAD58 (*virB4*::*phoA237*), pTAD59 (*virB4*::*phoA250*), and pTAD60 (*virB4*::*phoA312*), and *A. tumefaciens* cells carrying these plasmids ligated to the BHR vector pSW172, grew as white colonies on XP-containing plates. These strains possessed background levels of AP activity (0 to 2 U per OD_{600} unit) as determined by quantitative assay (Fig. 3B).

All of the active *virB4*::*phoA* and *virB5*::*phoA* gene fusions synthesized immunoreactive bands of the size expected for intact AP, and several synthesized immunoreactive species of sizes expected for the full-length hybrid proteins, as determined by immunoblot analysis (data not shown). Hybrid proteins joined at residues 237, 250, and 312 of VirB4 were undetectable, consistent with the notion that cytoplasmically disposed PhoA is rapidly degraded and is not accessible to binding by PhoA antibody. The correlation between AP activities and steady-state abundance of corresponding hybrid proteins suggests that differences in protein stabilities, not specific activities of PhoA moieties, account for the observed differences in AP activities. As noted below, the C terminus appears to have a stabilizing effect on native VirB4. The absence of these residues may prevent VirB4::PhoA hybrid proteins from adopting stable configurations.

Activities of *virB4*::*lacZ* fusions. We constructed a set of *virB4*::*lacZ* gene fusions by substituting *lacZ* for *'phoA* carried on the *virB4*::*phoA* gene fusions. Fig. 3C shows that the β-Gal activities of the β-Gal fusions were generally opposite the values of the AP activities of the corresponding PhoA fusions. Whereas VirB4::PhoA hybrid proteins joined at residues 237 and 780 exhibited background levels of PhoA activity, the corresponding VirB4::β-Gal hybrid proteins exhibited high β-Gal activities. Conversely, fusion of β-Gal at residues within regions 1 and 2 resulted in hybrid proteins with lower β-Gal activities. These findings are compatible with a VirB4 topology in which regions 1 and 2 correspond to exported domains and stretches of residues located between regions 1 and 2 and after region 2 correspond to cytoplasmic domains. It should be noted, however, that β-Gal activities of region 2 fusions were on the order of four- to fivefold higher than those of region 1 fusions. While this finding could raise a question as to whether region 2 indeed spans the membrane, a transmembrane configuration for this region is supported by results of protease susceptibility experiments (see below).

Protease susceptibility of VirB4. We complemented the reporter protein fusion experiments by assaying for effects of protease on the integrity of VirB4. Figure 5 shows that protease treatment of A348 whole cells had no effect on VirB4, but treatment of A348 spheroplasts resulted in degradation of the 87-kDa protein with the concomitant appearance of two immunoreactive species with apparent molecular sizes of ~45 and 35 kDa (Fig. 5A, lanes 5 to 7). Treatment of spheroplasts, but not whole cells, resulted in degradation of VirB5, but

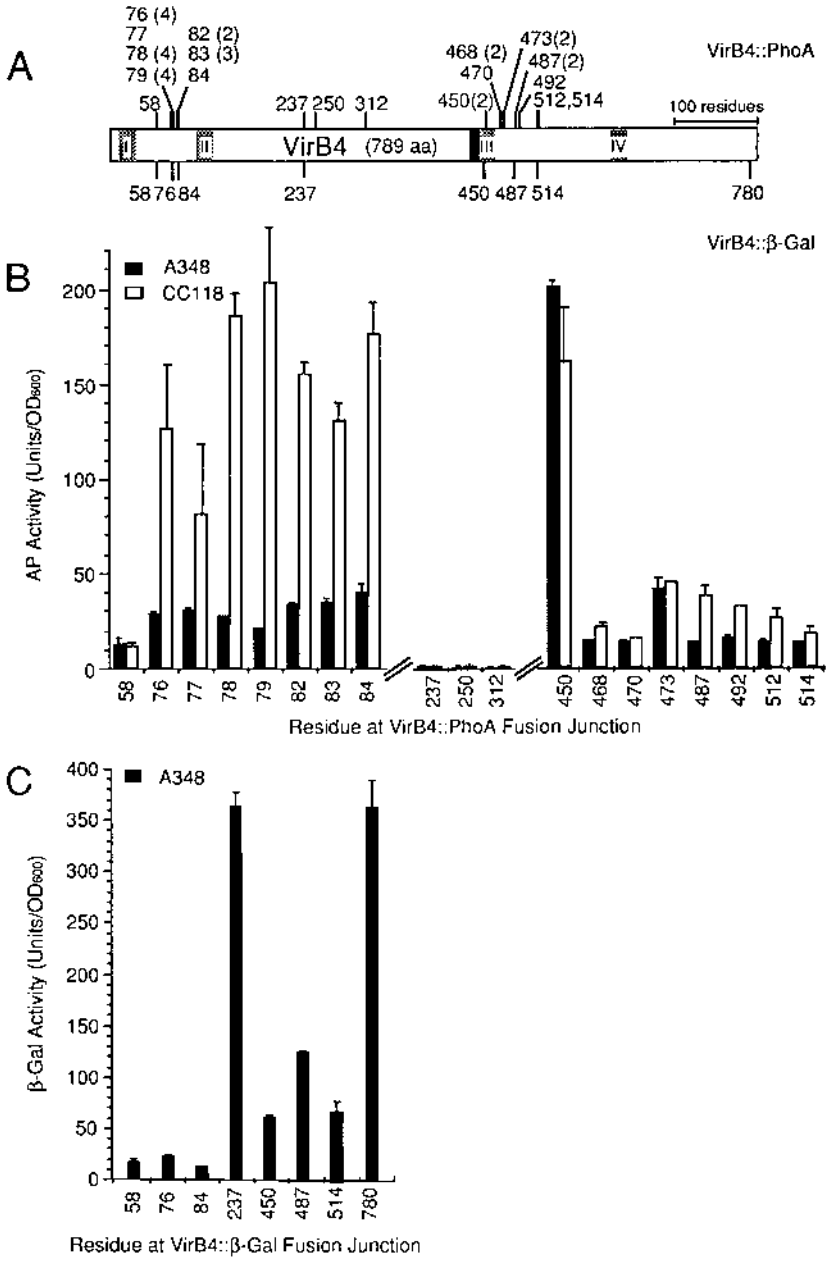

FIG. 3. AP and β-Gal activities of reporter protein fusions expressed in *E. coli* CC118 or *A. tumefaciens* A348. (A) Positions of the junction sites are identified according to the C-terminal-most amino acid residues of VirB4 (as defined by Ward et al. [56, 57]) prior to the PhoA or β-Gal sequence. The numbers in parentheses refer to numbers of gene fusions shown by sequence analysis to have the same junction site. The absence of a number in parentheses indicates that only one gene fusion was isolated. Fusions with junction sites at residues 237, 250, and 312 were constructed by cloning (see Table 1). Shaded boxes with Roman numerals I to IV refer to hydrophobic stretches with membrane-spanning potential. Region 1 was defined by VirB4::PhoA fusions with junction sites at residues 50 to 84. Region 2 was defined by fusions with junction sites at residues 450 to 514. The blackened box denotes the position of a consensus Walker A nucleotide-binding motif. (B) AP activities of the VirB4::PhoA fusions synthesized in *E. coli* CC118 and *A. tumefaciens* A348. (C) β-Gal activities of corresponding VirB4::β-Gal fusions synthesized in *A. tumefaciens* A348. Background AP and β-Gal activities of *E. coli* CC118 and *A. tumefaciens* A348 routinely were <2 U per OD_{600} unit. Assays were performed in triplicate, with standard deviations denoted by vertical error bars.

without the appearance of low-molecular-weight immunoreactive species (Fig. 5A). By contrast, treatment of spheroplasts did not degrade cytoplasmic DnaA or VirB11 (Fig. 5A); these findings are in agreement with previous data from this laboratory (18). Protease treatment of spheroplasts from a derivative of A348 expressing the *lac* operon from pLAFR2 (Table 1) also did not degrade cytoplasmic β-Gal (data not shown). These controls show that exogenous protease failed to gain access to cytoplasmic proteins under these experimental conditions. Furthermore, protease treatment of detergent-lysed spheroplasts resulted in the complete degradation of VirB4, VirB5, VirB11, and DnaA, demonstrating that these proteins are not intrinsically resistant to protease (Fig. 5A, lane 9). Finally, we were unable to visualize the 45- and 35-kDa immunoreactive species upon treatment of spheroplasts from the nonpolar *virB4* null mutant PC1004 or the Ti-plasmidless strain A136, which confirms that these species are degradation products of VirB4 (data not shown).

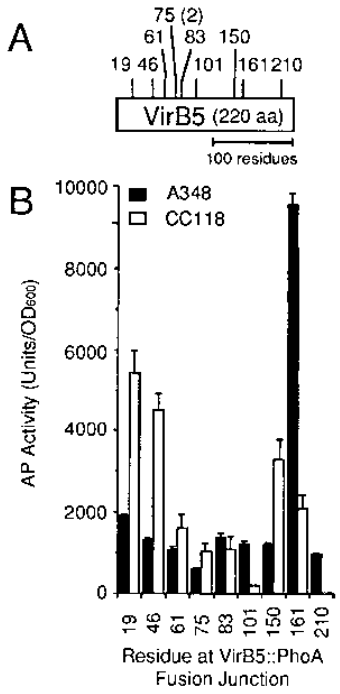

FIG. 4. AP activities of nine VirB5::PhoA fusions in *E. coli* CC118 and *A. tumefaciens* A348. (A) Positions of the junction sites are identified as described in the legend to Fig. 1. The numbers in parentheses refer to numbers of gene fusions identified by sequence analysis to have the same junction site. (B) AP activities of the VirB4::PhoA fusions synthesized in *E. coli* CC118 and *A. tumefaciens* A348. Assays were performed in triplicate, with standard deviations denoted by vertical error bars.

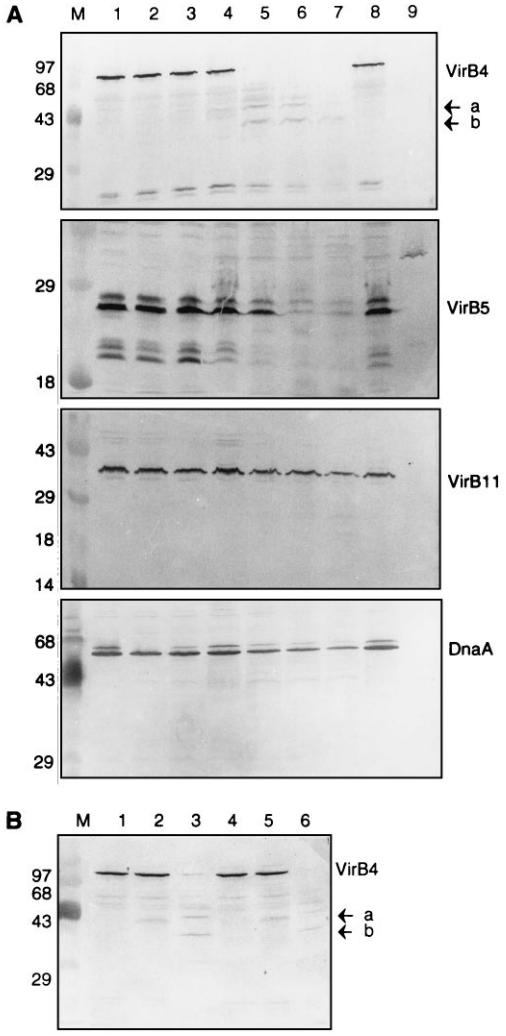

FIG. 5. Susceptibility of VirB4 to protease digestion in spheroplasts of *A. tumefaciens*. AS-induced *A. tumefaciens* strains A348 (A) and AS-induced and uninduced A348(pZDH10) (B) were converted to spheroplasts and treated with proteinase K as described in Materials and Methods. Treated samples were subjected to SDS-PAGE, and immunodevelopment of blots with the VirB4, VirB5, VirB11 and DnaA antisera was performed to identify the proteins listed at the right. (A) Lanes M, molecular mass standards, with sizes (in kilodaltons) listed at the left; lanes 1, whole cells without protease; lanes 2, whole cells with proteinase K added to 100 μg/ml; lanes 3, whole cells with PMSF added to 2 mM followed by addition of proteinase K to 100 μg/ml; lanes 4, spheroplasts without protease; lanes 5, spheroplasts with proteinase K added to 100 μg/ml; lanes 6, spheroplasts with proteinase K added to 200 μg/ml; lanes 7, spheroplasts with proteinase K added to 400 μg/ml; lanes 8, spheroplasts with PMSF added to 2 mM followed by addition of proteinase K to 400 μg/ml; lanes 9, lysed spheroplasts with proteinase K added to 100 μg/ml. (B) Lanes 1 to 3, AS-induced A348(pZDH10); lanes 4 to 6, uninduced A348(pZDH10); lanes 1 and 4, whole cells with proteinase K added to 400 μg/ml; lanes 2 and 5, spheroplasts without protease; lanes 3 and 6, spheroplasts with proteinase K added to 200 μg/ml. Arrows with lowercase letters a and b denote positions corresponding to ~45- and ~35-kDa immunoreactive species, respectively, that appeared upon protease treatment of A348 (panel A, lanes 5 to 7) and A348(pZDH10) (panel B, lanes 3 and 6) spheroplasts.

Figure 5B shows that treatment of spheroplasts from AS-induced and uninduced A348(pZDH10) cells also caused degradation of VirB4 with the concomitant appearance of the 45- and 35-kDa species, suggesting that similar domains are susceptible to protease in the presence and absence of *vir* gene products. The apparent molecular sizes of the immunoreactive species suggest that an extracytoplasmic domain is located near the middle of the protein, which is compatible with the identification of active VirB4::PhoA hybrid proteins with fusion sites mapping to region 2 (Fig. 3A). We gained additional evidence that both regions 1 and 2 of VirB4 are accessible to exogenous protease by demonstrating that the active VirB4::PhoA fusions with junction sites mapping in these regions were degraded upon protease treatment of spheroplasts (16). We attempted to further map the protease-susceptible regions of VirB4 by comparing the sizes of degradation products generated by proteolysis of several C-terminal truncation derivatives (Table 1). Each of these truncation derivatives accumulated at low levels. Although protease treatment of spheroplasts clearly caused degradation of these species, levels were not high enough to allow for immunological detection of degradation products (16).

DISCUSSION

In the present study, we evaluated the nature of the interaction of the VirB4 ATPase with the cytoplasmic membrane. Fractionation and membrane treatment studies provided evidence for a tight interaction with the membrane. The use of a nested-deletion strategy (52) led to the identification of enzymatically active VirB4::PhoA fusions that possessed junction sites in two discrete regions. A parallel analysis of VirB5, which has been predicted to localize peripherally at the periplasmic face of the cytoplasmic membrane (18, 20), led to identification of active VirB5::PhoA fusions with junction sites that mapped throughout the length of the protein. Although the VirB4::PhoA fusions exhibited lower activities than the

VirB5::PhoA fusions, the following three lines of evidence support the idea that the PhoA moieties joined at residues in regions 1 and 2 of VirB4 are exported across the cytoplasmic membrane. First, AP activities of strains synthesizing these hybrid proteins were well above background levels of host cells even with the addition of iodoacetamide prior to cell lysis; this sulfhydryl-alkylating agent has been shown to prevent formation of disulfide bonds and, hence, the proper folding of cytoplasmic PhoA (17). Second, AP activities generally were correlated with the abundance of VirB4::PhoA and VirB5::PhoA fusions. Strains synthesizing the VirB4::PhoA fusion proteins with junction sites in regions 1 and 2 accumulated immunoreactive polypeptides the size of native AP, and some accumulated detectable levels of the hybrid proteins. By contrast, the VirB4::PhoA fusions with junction sites outside of regions 1 and 2 were immunologically undetectable. Together, these findings suggest that the somewhat low AP activities of these fusion proteins most probably can be attributed to sensitivity to proteolysis. Consistent with this interpretation, analysis of truncation derivatives suggests that the C terminus of VirB4, which is missing in the hybrid proteins, contributes to protein stabilization (16). Third, VirB4::PhoA hybrid proteins with junction sites in regions 1 and 2 were degraded upon protease treatment of spheroplasts, whereas cytoplasmic markers were unaffected by these treatments. In addition to the evidence for export of PhoA moieties, results of the β-Gal fusion and protease susceptibility studies further support a transmembrane topology model for VirB4.

Region 1 is located near the N terminus of VirB4, between two potential membrane-spanning domains at residues 14 to 37 ($IYLPYIGH^+LSD^-H^+IVLLE^-D^-GSIMSIA$) (transmembrane domain I [TMI] and 108 to 131 ($VLSGQLLR^+ND^-H^+FLTLIVYPQAALG$) (TMII). Region 2 is near the middle of the protein, also between two potential membrane-spanning domains at residues 440 to 464 ($TLMMFV LAMLE^-QSMVD^-R^+AGTVVFF$) (TMIII) and 608 to 624 ($VCAPAAAYLLH^+R^+IGAMI$) (TMIV). It should be emphasized that the assignment of these potential TMs is based solely on the presence of sufficient numbers of contiguous hydrophobic residues to span the cytoplasmic membrane and on their proximities to junctions of active VirB4::PhoA fusion proteins. TMI and TMIII reside immediately upstream of region 1 and 2 junction points, respectively, which gives us confidence that these TMs are important for export of PhoA moieties of the active VirB4::PhoA fusion proteins. A previous sequence-based analysis also predicted that residues corresponding to TMI span the cytoplasmic membrane (6). The assignment of TMIV is less certain given that we failed to recover active hybrid proteins with junction points mapping between residue 514 and the beginning of TMIV. Interestingly, we identified one fusion protein, VirB4::PhoA450, with a junction point that mapped within TMIII (Fig. 3). In their studies of LacY permease, Calamia and Manoil (10) determined that as few as 9 to 11 amino acids of a larger membrane-spanning sequence are sufficient to promote PhoA export as long as they are contiguous apolar residues. Likewise, the junction point at residue 450 for VirB4::PhoA450 is located just after a stretch of 10 contiguous apolar residues within the larger putative transmembrane domain TMIII. In addition, it has been noted that fusion proteins with junctions in the latter half of an outgoing transmembrane stretch often exhibit high AP activities (10). This observation could account for the unusually high AP activity of the VirB4::PhoA450 fusion protein compared with the other VirB4::PhoA fusion proteins.

There are several potentially charged residues in TMI to TMIV. As mentioned above, a subset of as few as nine residues can suffice as a transmembrane segment, so it is possible that most of these charged residues are not embedded within the membrane. It may be of significance, however, that the net charge balance of TMI and TMII and that of TMIII and TMIV potentially approach zero and, furthermore, that four of the charged residues in TMI and the three in TMII lie on the same sides of the corresponding α helices, as predicted by the Wisconsin Genetics Computer Group Helicalwheel program. Similarly membrane-embedded charged residues within transmembrane α helices of other membrane proteins, such as bacteriorhodopsin and sensory rhodopsin I (see reference 48) and lactose permease (11), have been postulated to form salt bridges, for movement of ions, as critical features of the associated signalling and transport processes. Furthermore, an earlier study by Oosawa and Simon (38) showed that an A19K substitution in TMI of the Tar chemoreceptor of *E. coli* could be suppressed by substituting glutamic acid residues for hydrophobic residues in TMII. Together, these findings support the notion that charged residues within transmembrane regions are potential sites for establishment of domain interactions via formation of ion pairs. Thus, the presence of charged residues does not preclude insertion of TMI to TMIV of VirB4 into or through the cytoplasmic membrane. These residues may in fact play a critical role(s) in an unidentified charge transfer reaction(s) associated with T-complex transport.

TMIII immediately follows a consensus Walker A NTP-binding site, and TMIV is just before a potential Walker B motif surrounding an Asp residue at position 634. The identification of active VirB4::PhoA fusions with junctions mapping to region 2 raises the intriguing possibility that residues between these A and B motifs comprise an extracytoplasmic domain. Computer-assisted modeling studies (25, 36) and experimental findings for the HisP (1, 3) and MalK (44) ATPase subunits of the histidine and maltose transporters, respectively, have provided support for this possibility. Modeling studies based on the known structure of adenylate kinase have led to a prediction that the Walker A and B sites form a tightly folded core structure that binds and hydrolyzes ATP. The less-conserved, generally hydrophobic sequences between the A and B sites are depicted as single-loop (36) or two-loop (25) structures that extend from the core structure. Results of early genetic (1) studies of HisP and more recent protease susceptibility studies of HisP (3), MalK (44), and SecA (28) have also led to predictions that each of these transporter ATPases possesses a transmembrane topology. While further studies clearly are needed to better define the membrane configurations of these transporter ATPases, it may be relevant that a recombinant nucleotide-binding fold from the cystic fibrosis transmembrane regulator protein, a eukaryotic homolog of HisP and MalK, recently was shown to exhibit anion channel-forming activity when reconstituted into planar bilayers (2). This finding is at least consistent with the possibility that the nucleotide-binding folds of related transporter ATPases span the cytoplasmic membrane. On the basis of these observations, an intriguing speculation is that a hydrophobic loop(s) located just after the Walker A box of VirB4 embeds in or spans the cytoplasmic membrane. Such a transmembrane topology could facilitate interactions of VirB4 with other integral membrane components of the T-complex transport machinery. Alternatively, such a topology could provide a mechanism for transduction of information, in the form of ATP-dependent conformational changes, across the cytoplasmic membrane to periplasmic components of the transport machinery. As a test of these ideas, it will be of considerable interest to assay for interactions between this region of VirB4 and integral membrane or periplasmic components of the transport machinery.

Taken together, the results of our studies are consistent with a model which depicts VirB4 as a polytopic membrane protein with two periplasmic and three cytoplasmic domains. We suggest that the periplasmic domains coincide with regions 1 and 2 and that one of the cytoplasmic domains is located between regions 1 and 2 and the other is located between region 2 and the C terminus (Fig. 3A). The third cytoplasmic domain is at the extreme N terminus, as deduced from the observations that (i) a VirB4 derivative with a 2-kDa His-containing moiety at its N terminus is functionally indistinguishable from native VirB4; (ii) His-VirB4 is retained on an Ni^{2+} affinity column; and (iii) His-VirB4 migrates more slowly than does native VirB4 in SDS-polyacrylamide gels, most probably as a result of retention of the His tag (16). Overall, this proposed topology is in accordance with the positive-inside rule of von Heijne and Gavel: more positively charged residues are located in the cytoplasmic regions of VirB4 than in the translocated periplasmic regions (55). Also, positively charged residues are located next to the predicted cytoplasmic faces of the four TMs, which may influence the orientation of the TMs in the cytoplasmic membrane (15, 55).

Our studies do not exclude alternative topologies. For example, VirB4 could assemble as a component of the T-complex transport apparatus in such a way that the proposed periplasmic domains do not completely traverse the cytoplasmic membrane but rather embed only partially in the membrane in a way that would allow for the export of fused PhoA moieties and for accessibility to membrane-impermeant proteases. Proteases could gain access to domains of VirB4, for example, by first degrading other proteins that shield VirB4 from the periplasmic surface. A second intriguing possibility, also offered as an explanation for the protease susceptibilities of SecA, HisP, and MalK (3, 28, 44), is that proteases selectively degrade domains of VirB4 that are exposed within the transport channel.

Results of the present investigations failed to reveal any influence of other Vir proteins on the membrane topology of VirB4. It should be noted, however, that previous results from our laboratory indicate that VirB4 is in fact stabilized at the membrane through interactions with other VirB proteins (8, 19). Thus, more sensitive assays must be used to ascertain if VirB4 undergoes conformation changes as a result of such stabilizing protein interactions. Moreover, further studies are needed to examine the influence of ATP binding or hydrolysis on membrane configuration. It is noteworthy that the SecA ATPase, like VirB4, exhibits protease susceptibility patterns that are indistinguishable in the presence and absence of two stabilizing factors, SecD and SecF. Yet, SecA exists in an ATP-dependent, dynamic association with the cytoplasmic membrane (28).

Of the VirB4 homologs associated with macromolecular transport, extensive structural studies have been carried out only for TraC, a presumed component of the F plasmid conjugation apparatus (42). Similar to VirB4, TraC associates with the cytoplasmic membrane despite its overall hydrophilic character; furthermore, the N terminus of TraC also is not processed (43). However, the membrane association of TraC is dependent on synthesis of other Tra proteins. Moreover, a mutant derivative, TraC1044, which contains an Arg-to-Cys mutation at residue 811, was shown to exhibit a weaker membrane interaction than does native TraC, suggesting that TraC possesses a C-terminal domain which is directly responsible for interaction with the membrane or with an integral membrane protein(s) (43). Our studies provide strong evidence that membrane interaction domains map elsewhere in VirB4. It is noteworthy, however, that both the deletion of certain VirB proteins from cells (8) and the deletion of C-terminal residues of VirB4 (16) have the same phenotypic consequence, namely, VirB4 destabilization. These observations raise the intriguing possibility that determinants localized at the C terminus are required for establishment of stabilizing interactions with other components of the T-complex transport machinery.

TraC has been postulated to be involved in assembly (and perhaps disassembly) of F pilus proteins into mature structures (43). Recently, Fullner et al. (21) made the important discovery that the VirB proteins also assemble into a pilus structure, but a morphogenetic role for VirB4 per se could not be established since each of the strains deleted of a single *virB* gene failed to assemble pili. We have shown that a strain sustaining a nonpolar *virB4* null mutation accumulates wild-type levels of other VirB proteins (8). In striking contrast, mutants with nonpolar deletions of several other *virB* genes, e.g., *virB6*, *virB7*, and *virB9*, accumulate strongly diminished levels of other VirB proteins (8, 19). On the basis of these findings, we have postulated that proteins such as VirB6, VirB7, and VirB9 play important morphogenetic roles in the assembly of VirB proteins into a stabilized transporter/pilus (19, 47). Although there is evidence that VirB4 promotes stabilization of VirB3 (26), its apparent lack of involvement in the general stabilization of other VirB proteins leads us to suggest that VirB4 probably does not play a central role in transporter biogenesis. Instead, we propose that VirB4 couples the energy of ATP hydrolysis to substrate translocation by a mechanism which is critically dependent on a transmembrane topology.

ACKNOWLEDGMENTS

We thank Tsz Kwong Man for helpful discussions and excellent technical assistance with the AP assays and Michelle Filppen for technical assistance with the PhoA mutagenesis. We thank Svetlana Rashkova, Xue-Rong Zhou, and John Spudich for helpful discussions and Kathy Borkovich for helpful discussions and for critical reading of the manuscript. We thank George Weinstock and Jesus Eraso for plasmid constructs and William Margolin and Steve Winans for the DnaA and VirA antibodies, respectively.

This work was supported by NIH grant GM48746 to P.J.C.

REFERENCES

1. **Ames, G. F.-L., and E. N. Spudich.** 1976. Protein-protein interactions in transport: periplasmic histidine binding protein J interacts with P protein. Proc. Natl. Acad. Sci. USA **73:**1877–1881.
2. **Arispe, N., E. Rojas, J. Hartman, E. J. Sorscher, and H. B. Pollard.** 1992. Intrinsic anion channel activity of the recombinant first nucleotide binding fold domain of the cystic fibrosis transmembrane regulator protein. Proc. Natl. Acad. Sci. USA **89:**1539–1543.
3. **Baichwal, V., D. Liu, and G. F. Ames.** 1993. The ATP-binding component of a prokaryotic traffic ATPase is exposed to the periplasmic (external) surface. Proc. Natl. Acad. Sci. USA **90:**620–624.
4. **Balzer, D., W. Pansegrau, and E. Lanka.** 1994. Essential motifs of relaxase (TraI) and TraG proteins involved in conjugative transfer of plasmid RP4. J. Bacteriol. **176:**4285–4295.
5. **Beijersbergen, A., A. D. Dulk-Ras, R. A. Schilperoort, and P. J. J. Hooykaas.** 1992. Conjugative transfer by the virulence system of *Agrobacterium tumefaciens*. Science **256:**1324–1327.
6. **Beijersbergen, A., S. J. Smith, and P. J. J. Hooykaas.** 1994. Localization and topology of VirB proteins of *Agrobacterium tumefaciens*. Plasmid **32:**212–218.
7. **Berger, B. R., and P. J. Christie.** 1993. The *Agrobacterium tumefaciens virB4* gene product is an essential virulence protein requiring an intact nucleoside triphosphate-binding domain. J. Bacteriol. **175:**1723–1734.
8. **Berger, B. R., and P. J. Christie.** 1994. Genetic complementation analysis of the *Agrobacterium tumefaciens virB* operon: *virB2* through *virB11* are essential virulence genes. J. Bacteriol. **176:**3646–3660.
9. **Binns, A. N., C. E. Beaupré, and E. M. Dale.** 1995. Inhibition of VirB-mediated transfer of diverse substrates from *Agrobacterium tumefaciens* by the IncQ plasmid RSF1010. J. Bacteriol. **177:**4890–4899.
10. **Calamia, J., and C. Manoil.** 1990. *lac* permease of *Escherichia coli*: topology and sequence elements promoting membrane insertion. Proc. Natl. Acad. Sci. USA **87:**4937–4941.
11. **Calamia, J., and C. Manoil.** 1992. Membrane protein spanning segments as

export signals. J. Mol. Biol. **224:**539–543.
12. **Chen, C.-Y., and S. C. Winans.** 1991. Controlled expression of the transcriptional activator gene *virG* in *Agrobacterium tumefaciens* by using the *Escherichia coli lac* promoter. J. Bacteriol. **173:**1139–1144.
13. **Christie, P. J., J. E. Ward, M. P. Gordon, and E. W. Nester.** 1989. A gene required for transfer of T-DNA to plants encodes an ATPase with autophosphorylating activity. Proc. Natl. Acad. Sci. USA **86:**9677–9681.
14. **Christie, P. J., J. E. Ward, S. C. Winans, and E. W. Nester.** 1988. The *Agrobacterium tumefaciens virE2* gene product is a single-stranded-DNA-binding protein that associates with T-DNA. J. Bacteriol. **170:**2659–2667.
15. **Dalbey, R. E.** 1990. Positively charged residues are important determinants of membrane protein topology. Trends Biochem. Sci. **15:**253–257.
16. **Dang, T. A., and P. J. Christie.** Unpublished data.
17. **Derman, A. I., and J. Beckwith.** 1995. *Escherichia coli* alkaline phosphatase localized to the cytoplasm slowly acquires enzymatic activity in cells whose growth has been suspended: a caution for gene fusion studies. J. Bacteriol. **177:**3764–3770.
18. **Fernandez, D., T. A. T. Dang, G. M. Spudich, X.-R. Zhou, B. R. Berger, and P. J. Christie.** 1996. The *Agrobacterium tumefaciens virB7* gene product, a proposed component of the T-complex transport apparatus, is a membrane-associated lipoprotein exposed at the periplasmic surface. J. Bacteriol. **178:** 3156–3167.
19. **Fernandez, D., G. M. Spudich, X.-R. Zhou, and P. J. Christie.** 1996. The *Agrobacterium tumefaciens* VirB7 lipoprotein is required for stabilization of VirB proteins during assembly of the T-complex transport apparatus. J. Bacteriol. **178:**3168–3176.
20. **Finberg, K. E., T. R. Muth, S. P. Young, J. B. Maken, S. M. Heitritter, A. N. Binns, and L. M. Banta.** 1995. Interactions of VirB9, -10, and -11 with the membrane fraction of *Agrobacterium tumefaciens*: solubility studies provide evidence for tight associations. J. Bacteriol. **177:**4881–4889.
21. **Fullner, K. J., J. C. Lara, and E. W. Nester.** 1996. Pilus assembly by *Agrobacterium* T-DNA transfer genes. Science **273:**1107–1109.
22. **Fullner, K. J., K. M. Stephens, and E. W. Nester.** 1994. An essential virulence protein of *Agrobacterium tumefaciens*, VirB4, requires an intact mononucleotide binding domain to function in transfer of T-DNA. Mol. Gen. Genet. **245:**704–715.
23. **Garfinkel, D. J., R. B. Simpson, L. W. Ream, F. F. White, M. P. Gordon, and E. W. Nester.** 1981. Genetic analysis of crown gall: fine structure map of the T-DNA by site-directed mutagenesis. Cell **27:**143–153.
24. **Helenius, A., and K. Simons.** 1975. Solubilization of membranes by detergents. Biochim. Biophys. Acta **415:**29–79.
25. **Hyde, S. C., P. Emsley, M. J. Hartshorn, M. M. Mimmack, U. Gileadi, S. R. Pearce, M. P. Hallagher, D. R. Gill, R. E. Hubbard, and C. F. Higgins.** 1990. Structural model of ATP-binding proteins associated with cystic fibrosis, multidrug resistance and bacterial transport. Nature **346:**362–365.
26. **Jones, A. L., K. Shirasu, and C. I. Kado.** 1994. The product of the *virB4* gene of *Agrobacterium tumefaciens* promotes accumulation of VirB3 protein. J. Bacteriol. **176:**5255–5261.
27. **Kado, C. I.** 1993. *Agrobacterium*-mediated transfer and stable incorporation of foreign genes in plants, p. 243–254. *In* D. B. Clewell (ed.), Bacterial conjugation. Plenum Press, New York, N.Y.
28. **Kim, Y. J., T. Rajapandi, and D. Oliver.** 1994. SecA protein is exposed to the periplasmic surface of the *E. coli* inner membrane in its active state. Cell **78:**845–853.
29. **Kuldau, G. A., G. DeVos, J. Owen, G. McCaffrey, and P. Zambryski.** 1990. The *virB* operon of *Agrobacterium tumefaciens* pTiC58 encodes 11 open reading frames. Mol. Gen. Genet. **221:**256–266.
30. **Lessl, M., D. Balzer, W. Pansegrau, and E. Lanka.** 1992. Sequence similarities between the RP4 Tra2 and the Ti VirB region strongly support the conjugation model for T-DNA transfer. J. Biol. Chem. **267:**20471–20480.
31. **Lessl, M., and E. Lanka.** 1994. Common mechanisms in bacterial conjugation and Ti-mediated T-DNA transfer to plant cells. Cell **77:**321–324.
32. **Lessl, M., W. Pansegrau, and E. Lanka.** 1992. Relationship of DNA-transfer systems: essential transfer factors of plasmids RP4, Ti, and F share common sequences. Nucleic Acids Res. **20:**6099–6100.
33. **Manoil, C.** 1991. Analysis of membrane protein topology using alkaline phosphatase and β-galactosidase gene fusions. Methods Cell Biol. **34:**61–75.
34. **Margolin, W., D. Bramhill, and S. R. Long.** 1995. The *dnaA* gene of *Rhizobium meliloti* lies within an unusual gene arrangement. J. Bacteriol. **177:** 2892–2900.
35. **Miller, J. H.** 1972. Experiments in molecular genetics. Cold Spring Harbor Laboratory, Cold Spring Harbor, N.Y.
36. **Mimura, C. S., S. R. Holbrook, and G. F.-L. Ames.** 1991. Structural model of the nucleotide-binding conserved component of periplasmic permeases. Proc. Natl. Acad. Sci. USA **88:**84–88.
37. **Okamoto, S., A. Toyoda-Yamamoto, K. Ito, I. Takebe, and Y. Machida.** 1991. Localization and orientation of the VirD4 protein of *Agrobacterium tumefaciens* in the cell membrane. Mol. Gen. Genet. **228:**24–32.
38. **Oosawa, K., and M. Simon.** 1986. Analysis of mutations in the transmembrane region of the aspartate chemoreceptor in *Escherichia coli*. Proc. Natl. Acad. Sci. USA **83:**6930–6934.
39. **Pohlman, R. F., H. D. Genetti, and S. C. Winans.** 1994. Common ancestry between IncN conjugal transfer genes and macromolecular export systems of plant and animal pathogens. Mol. Microbiol. **14:**655–668.
40. **Rashkova, S., G. M. Spudich, and P. J. Christie.** Characterization of membrane and protein interaction determinants of the *Agrobacterium tumefaciens* VirB11 ATPase. J. Bacteriol., in press.
41. **Sambrook, J., E. F. Fritsch, and T. Maniatis.** 1989. Molecular cloning: a laboratory manual, 2nd ed. Cold Spring Harbor Laboratory, Cold Spring Harbor, N.Y.
42. **Schandel, K. A., S. Maneewannakul, R. A. Vonder Haar, K. Ippen-Ihler, and R. E. Webster.** 1990. Nucleotide sequence of the F plasmid gene, *traC*, and identification of its product. Gene **96:**137–140.
43. **Schandel, K. A., M. M. Muller, and R. E. Webster.** 1992. Localization of TraC, a protein involved in assembly of the F conjugative pilus. J. Bacteriol. **174:**3800–3806.
44. **Schneider, E., S. Hunke, and S. Tebbe.** 1995. The MalK protein of the ATP-binding cassette transporter for maltose of *Escherichia coli* is accessible to protease digestion from the periplasmic side of the membrane. J. Bacteriol. **177:**5364–5367.
45. **Shirasu, K., Z. Koukolikova-Nicola, B. Hohn, and C. I. Kado.** 1994. An inner-membrane-associated virulence protein essential for T-DNA transfer from *Agrobacterium tumefaciens* to plants exhibits ATPase activity and similarities to conjugative transfer genes. Mol. Microbiol. **11:**581–588.
46. **Shirasu, K., P. Morel, and C. I. Kado.** 1990. Characterization of the *virB* operon of an *Agrobacterium tumefaciens* Ti plasmid: nucleotide sequence and protein analysis. Mol. Microbiol. **4:**1153–1163.
47. **Spudich, G. M., D. Fernandez, X.-R. Zhou, and P. J. Christie.** 1996. Intermolecular disulfide bonds stabilize VirB7 homodimers and VirB7/VirB9 heterodimers during biogenesis of the *Agrobacterium tumefaciens* T-complex transport apparatus. Proc. Natl. Acad. Sci. USA **93:**7512–7517.
48. **Spudich, J. L.** 1994. Protein-protein interaction converts a proton pump into a sensory receptor. Cell **79:**747–750.
49. **Stachel, S. E., and E. W. Nester.** 1986. The genetic and transcriptional organization of the *vir* region of the A6 Ti plasmid of *Agrobacterium tumefaciens*. EMBO J. **4:**1445–1454.
50. **Stachel, S. E., and P. C. Zambryski.** 1986. *Agrobacterium tumefaciens* and the susceptible plant cell: a novel adaptation of extracellular recognition and DNA conjugation. Cell **47:**155–157.
51. **Stephens, K. M., C. Roush, and E. Nester.** 1995. *Agrobacterium tumefaciens* VirB11 protein requires a consensus nucleotide-binding site for function in virulence. J. Bacteriol. **177:**27–36.
52. **Sugiyama, J. E., S. Mahmoodian, and G. R. Jacobson.** 1991. Membrane topology analysis of *Escherichia coli* mannitol permease by using a nested deletion method to create *mtlA-phoA* fusions. Proc. Natl. Acad. Sci. USA **88:**9603–9607.
53. **Thompson, D. V., L. S. Melchers, K. B. Idler, R. A. Schilperoort, and P. J. J. Hooykaas.** 1988. Analysis of the complete nucleotide sequence of the *Agrobacterium tumefaciens virB* operon. Nucleic Acids Res. **16:**4621–4636.
54. **Tummuru, M. K. R., S. A. Sharma, and M. J. Blaser.** 1995. *Helicobacter pylori picB*, a homologue of the *Bordetella pertussis* toxin secretion protein, is required for induction of IL-8 in gastric epithelial cells. Mol. Microbiol. **18:**867–876.
55. **von Heijne, G., and Y. Gavel.** 1988. Topogenic signals in integral membrane proteins. Eur. J. Biochem. **174:**671–678.
56. **Ward, J. E., D. E. Akiyoshi, D. Regier, A. Datta, M. P. Gordon, and E. W. Nester.** 1988. Characterization of the *virB* operon from an *Agrobacterium tumefaciens* Ti plasmid. J. Biol. Chem. **263:**5804–5814.
57. **Ward, J. E., D. E. Akiyoshi, D. Regier, A. Datta, M. P. Gordon, and E. W. Nester.** 1990. Characterization of the *virB* operon from an *Agrobacterium tumefaciens* Ti plasmid. J. Biol. Chem. **265:**4768. (Author's correction.)
58. **Ward, J. E., Jr., E. M. Dale, P. J. Christie, E. W. Nester, and A. N. Binns.** 1990. Complementation analysis of *Agrobacterium tumefaciens* Ti plasmid *virB* genes by use of a *vir* promoter expression vector: *virB9*, *virB10*, and *virB11* are essential virulence genes. J. Bacteriol. **172:**5187–5199.
59. **Watson, B., T. C. Currier, M. P. Gordon, M.-D. Chilton, and E. W. Nester.** 1975. Plasmid required for virulence of *Agrobacterium tumefaciens*. J. Bacteriol. **123:**255–264.
60. **Weiss, A. A., F. D. Johnson, and D. L. Burns.** 1993. Molecular characterization of an operon required for pertussis toxin secretion. Proc. Natl. Acad. Sci. USA **90:**2970–2974.
61. **Winans, S. C., D. L. Burns, and P. J. Christie.** 1996. Adaptation of a conjugal transfer system for the export of pathogenic macromolecules. Trends Microbiol. **4:**1616–1622.
62. **Winans, S. C., R. A. Kerstetter, J. E. Ward, and E. W. Nester.** 1989. A protein required for transcriptional regulation of *Agrobacterium* virulence genes spans the cytoplasmic membrane. J. Bacteriol. **171:**1616–1622.
63. **Zambryski, P. C.** 1992. Chronicles from the *Agrobacterium*-plant cell DNA transfer story. Annu. Rev. Plant Physiol. Plant Mol. Biol. **43:**465–490.
64. **Zupan, J. R., and P. Zambryski.** 1995. Transfer of T-DNA from *Agrobacterium* to the plant cell. Plant Physiol. **107:**1041–1047.